ORIGINAL RESEARCH ARTICLE

Mechanical Properties of Recycled Carbon Fiber-Reinforced Resin Composites 3D Printed via Digital Light Processing

Frederico de Castro Magalhães ⓘ and Juan Carlos Campos Rubio

Additive manufacturing, particularly with UV-curable resin-based 3D printing, has revolutionized production processes, allowing precise fabrication of intricate geometries. However, challenges persist in composite printing, particularly in meeting the demand for second-life applications due to the considerable volume of carbon fiber waste. This study addresses this issue by researching the compatibility of mechanically produced recyclable carbon fibers with UV-curable resin. The short carbon fibers were combined with the resin at varying weight percentages (1.5, 3, 6, 9, 12, and 15 wt.%) to determine the optimal ratio for achieving maximum Young's modulus and tensile strength in resulting composites. Utilizing digital light processing (DLP) 3D printing technology, the study systematically evaluated composite roughness, surface hardness, and voids volume. Each 3 wt.% increase in recycled carbon fiber concentration within the UV-curable resin resulted in a 0.01 g/cm^3 density decrease, accompanied by a 0.02 μm increase in surface roughness, with no impact on hardness. Notably, the 3 wt.% concentration proved optimal, exhibiting a 27% increase in Young's modulus and a 44% increase in tensile strength compared to the pure resin.

1. Introduction

Additive manufacturing has revolutionized production processes, allowing for the creation of complex geometries with remarkable precision. Within this realm, 3D printing employing UV-curable resin, including methods such as stereolithography (SLA), digital light processing (DLP), continuous liquid interface production (CLIP), and selective laser densification (SLD), has gained prominence. Despite their advantages in producing intricate designs, resin-based printing encounters challenges, particularly in the context of printing composites such as carbon fiber. The prohibitive cost of carbon fiber restricts its application in advanced contexts, prompting a closer examination of sustainable practices, including recycling methods.

However, the high cost of carbon fiber often restricts its application in certain advanced and high-performance contexts. For instance, the global demand for carbon fiber composites in the aerospace industry (wings, airframes and tail sections) is approximately 32%, followed by the automotive industry (rooftop, for example) at 21.5%. With carbon fiber production reaching 150,000 tons in 2021 (Ref 1) and an estimated 31,000 tons of carbon fiber-reinforced composites entering landfills annually (Ref 2), it becomes evident that the demand for second-life applications is now more critical than ever. The escalating demand for carbon fiber is anticipated to exceed global supply by the year 2030 (Ref 3, 4), notwithstanding the fact that around 30% of all virgin carbon fiber is discarded as material offcuts. Additionally, carbon fibers are derived from unsustainable fossil-based materials through energy-intensive processes."

The recycling of carbon fiber waste, which includes virgin offcuts and expired materials, involves two primary methodologies. Mechanically based recycling entails breaking down the waste through processes like crushing or milling, followed by sieving and classification into fine and coarse recyclate products (Ref 5). The alternative approach is thermal recycling, commonly known as pyrolysis or oxidation, extensively employed to reclaim carbon fiber-reinforced polymer composites. This thermal process involves the controlled decomposition of organic molecules through heating within a chemically inert environment. However, recycling processes for carbon fibers may have detrimental effects on their mechanical properties, potentially resulting in reductions of up to 13 and 85% in tensile modulus and tensile strength, respectively (Ref 6). Furthermore, it is imperative to assess the interaction between rec'yclable fibers and the polymeric matrix and thoroughly scrutinize the subsequent performance of reprocessed carbon fiber composites. Therefore, it is crucial to explore new routes for the reuse of short carbon fibers and investigate the resulting performance of reprocessed composites.

Reclaimed carbon fiber, obtained through recycling or upcycling of carbon fiber waste, is available in various forms, including non-woven fabrics, large chopped fibers (>1 cm),

Frederico de Castro Magalhães and **Juan Carlos Campos Rubio**, Department of Mechanical Engineering, Federal University of Minas Gerais, Belo Horizonte, Brazil. Contact e-mail: fredmag@demec.ufmg.br.

and very short fibers, typically less than 1 mm in length. The term " short carbon fiber" specifically denotes carbon fibers with a length of less than 1 mm. Presently, there is no standardized terminology utilized in existing literature for these sub-1000 μm carbon fibers, leading to the interchangeable use of terms such as "milled," "powdered," and "short carbon fiber" (Ref 7).

The compatibility of the chosen reinforcement materials with the UV-curable resin may influence the printing process and the final properties of the composites. Eyckens et al. (Ref 8) and Randall et al. (Ref 9) explore the challenges associated with material selection and compatibility, highlighting the need for further research to optimize the interaction between the reinforcement materials and the UV-curable resin. Additionally, the use of UV-curable resin enables the production of lightweight components with excellent mechanical properties. This is evident in works like He et al. (Ref 10) and Karimi and Javadpour (Ref 11), where high-strength and stiff carbon fiber composites and glass fiber-reinforced composites were achieved, respectively.

Achieving a uniform dispersion and distribution of reinforcement materials within the resin matrix proves challenging, as discussed by Yukako et al. (Ref 12) and Yamamoto et al. (Ref 13). The anisotropic nature of printed composites imposes limitations on applications that demand consistent mechanical behavior in all directions, stemming from challenges in controlling material dispersion during the printing process. Additionally, the printability of specific carbon fiber composites (Ref 14), especially those with a high loading of reinforcing materials, may be impeded by the viscosity and flow properties of the UV-curable resin. High-viscosity resins can compromise material dispersion, as demonstrated in studies by Lee et al. (Ref 15) and Katogi et al. (Ref 16), highlighting the potential for intricate structural designs.

Concerning the length of carbon fibers, Rahmani et al. (Ref 17) evaluated two types of continuous carbon fibers to determine the ideal volume fraction for predicting Young's modulus and tensile strength. Meanwhile, Mahat et al. (Ref 18) investigated the influence of curing time on the mechanical properties of carbon fiber-reinforced composites. In these perspectives, these studies did not explore changes in mechanical properties and void content when recyclable carbon fibers are employed as reinforcements in UV resins in low-cost 3D printers.

One advantage lies in the potential functionalization and customization of composite materials. Eng et al. (Ref 19) and Hu et al. (Ref 20) explore the functionalization of carbon fiber and glass fiber composites through 3D printing. This allows tailoring the properties of printed objects for specific applications, such as enhancing electrical conductivity. Various fillers like carbon nanotubes, graphene, and clay are dispersed in photopolymer UV-curable resin to enhance mechanical properties. Carbon fiber addition generally increases the stiffness of printed composites, with the Young's modulus rising by approximately 60% (Ref 21). Cholake et al. (Ref 22) demonstrated enhanced strength and stiffness by incorporating carbon fiber into printed parts, increasing the fatigue and tensile strength of epoxy composite by 11 and 22% with 2 wt.% of carbon fiber.

The industry trend toward new materials includes the prominent use of short carbon fiber, offering exceptional tensile strength, Young's modulus, low density, corrosion resistance, and lightweight properties (Ref 21). Short carbon fiber can replace traditional glass fiber to reinforce composites with UV-curable resin for rapid tooling. This approach effectively utilizes waste materials, as short carbon fiber can be mechanically mixed with UV-curable resin and printed by SLA printers, improving manufacturing efficiency (Ref 22).

In addition to mechanical properties, surface roughness and hardness are crucial for determining the quality and functionality of 3D printed parts. Surface roughness affects appearance, performance, and interaction, while hardness provides insights into durability and wear resistance.

This study utilized a liquid crystal display with selective digital light processing (DLP) technology to assess a photopolymer resin mixed with short carbon fiber (average length of 38 μm). The fabrication process, employing a bottom-up DLP-based photopolymerization platform, incorporated different weight percentages of short carbon fiber (1.5, 3, 6, 9, 12, and 15 wt.%) into the resin while maintaining a printer layer thickness of 50 μm. The aim was to evaluate the optimal weight percentage for higher Young's modulus and tensile strength, along with assessing the influence on roughness and hardness in the printed composites.

2. Materials and Methods

2.1 Specimen Manufacturing

For this study, specimens were fabricated using the Halot Sky SLA 3D printer manufactured by Creality, Inc. To initiate the printing process, 3D CAD data generated in Solidworks 2018 software were converted to STL format. Subsequently, the Halot Box 3.5.6 slicer software was utilized to slice the design into individual layers. Based on the sliced data, the UV-curable resin was cured by controlling the wavelength at 405 nm. The first layer was exposed for 70 seconds, while the normal exposure time for subsequent layers was set to 10 seconds. The layer resolution was maintained at 0.05 mm. For each composition, comprising pure resin and varying weight percentages of short carbon fiber, five specimens were printed normal to the build direction to ensure the accuracy and reliability of the results. Figure 1 illustrates the positions of the specimens in the 3D printing setup.

Initially, specimens were printed using solely translucent UV-curable resin (Anycubic), without the addition of short carbon fiber. Approximately 320 grams (equivalent to $\sim$ 300 ml) of the resin were used. Before printing, short carbon fiber rod measuring 38 μm length and 8.5 μm diameter (aspect ratio 4.47), obtained from Shezen Jingzhiyuan Carbon-Graphite Materials Co., Ltd., was immersed in a 2 wt.% ethanol solution for 2 hours. The ethanol solution was then evaporated at 80 °C until the powder was dried, ensuring improved interface bonding performance. The mechanical and physical properties of UV-curable resin and short carbon fiber are listed in Table 1.

Subsequently, the short carbon fiber was randomly introduced to the photopolymer resin and mechanically mixed in a planetary mixer for 5 minutes. Six different concentrations of short carbon fiber (1.5, 3, 6, 9, 12, and 15 wt.%) were evaluated to determine the optimal concentration to provide the highest value of Young's modulus and tensile strength.

Following the completion of the printing process, all specimens were detached from the printing head and immersed in a bath containing 99.9% isopropanol for 15 minutes. This step was performed to remove any unreacted resin and residual short carbon fiber. In accordance with the study conducted by
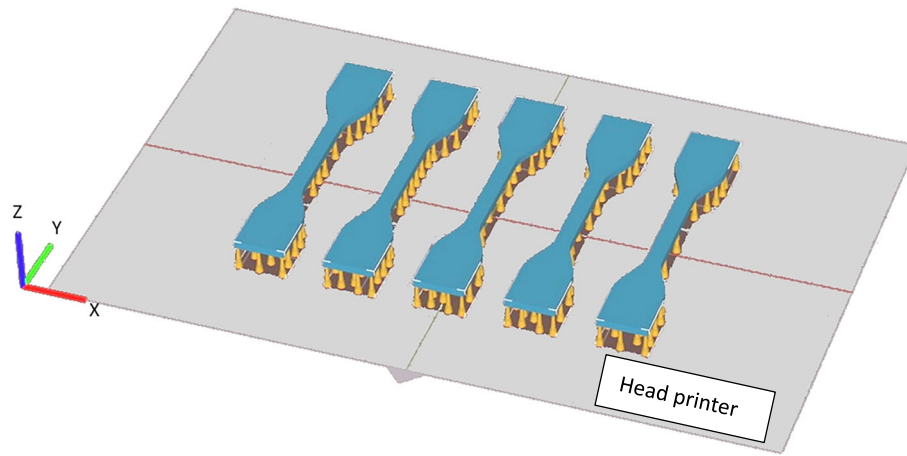
Fig. 1 Position of the specimens in the head printer to be printed

Table 1 Comparative physical and mechanical of UV-curable resin and short carbon fiber

	Density, g/cm^3	Viscosity, mPa s	Young's modulus, GPa	Tensile strength, MPa	Elongation at break, %
UV-curable resin standard	1.1	500	2.9–3.2	20−40	4−8
Short carbon fiber	1.6–1.76		30−35	800−850	1.6−2.2

Salih et al. (Ref 23), for components with small dimensions and simple geometries, such as the specimens employed in this investigation, a curing time of 10 minutes proves to be sufficient to conclude the manufacturing process.

2.2 Surface Roughness

The surface roughness (Ra) of each specimen's last printed layer was evaluated using a contact rugosimeter, specifically the Taylor Hobson Precision instrument. The accuracy of the rugosimeter was periodically verified using a calibration block. To measure the surface roughness (Ra) on the final printed layer, a cut-off value of 0.8 mm was employed, with a scanning speed of 1 mm/s and an evaluation length of 4 mm, following the guidelines specified in the ISO 4288-1996 standard. This measurement procedure was conducted at five different locations on each specimen, generating five individual Ra values. The average Ra value, calculated from these five measurements, represents the final Ra value for each test specimen.

2.3 Hardness

The hardness test was performed on the specimens according to the ASTM D2240 standard at room temperature. Each test specimen underwent measurements at five different locations on the last printed layer using a Shore D hardness tester. To evaluate the possible sedimentation of recyclable carbon fibers, hardness measurements were carried out at five specific points on both the upper and lower surfaces of the prints. The final hardness value for each specimen was determined by calculating the average of these measurements.

2.4 Tensile Test

The tensile tests were carried out using an AGS-X100kN Shimadzu testing machine at room temperature. The tests were performed on specimens without short carbon fiber (pure resin) as well as specimens containing different weight percentages of short carbon fiber. The crosshead speed during the tests was set to 1.00 mm/min, and no preload was applied.

The dimensions of the specimens, both for the pure resin and the composites with varying weight percentages of short carbon fiber, were prepared following the ASTM standard D638, as depicted in Fig. 2. The applied force versus extension of the specimens was continuously recorded until each sample failed. It is worth noting that no tabs were utilized in the specimens, and the fractures occurred within the gauge length.

The Young's modulus and tensile strength were calculated using the standard method. For each resin type (pure resin and composites with different weight percentages of short carbon fiber), five specimens were 3D printed and tested to ensure the statistical validity and accuracy of the results.

3. Results and Discussions

3.1 3D Printed Composites

The mechanical properties are significantly influenced by the dispersion, distribution in the matrix, and the weight percentage of short carbon fiber. When the distance between short carbon fibers is small, and they are evenly distributed without clustering, the reinforcement can create more sites for arresting crack/micro-crack growth. This implies that, for cracks to initiate, the system must go through multiple stages of initiation (resulting in high energy absorption) and subsequent propagation modes, thereby enhancing the fracture properties of the composite (Ref 21).

Despite having a diameter of approximately 8.5 μm, which is not as small as nanomaterials, short carbon fiber tends to face
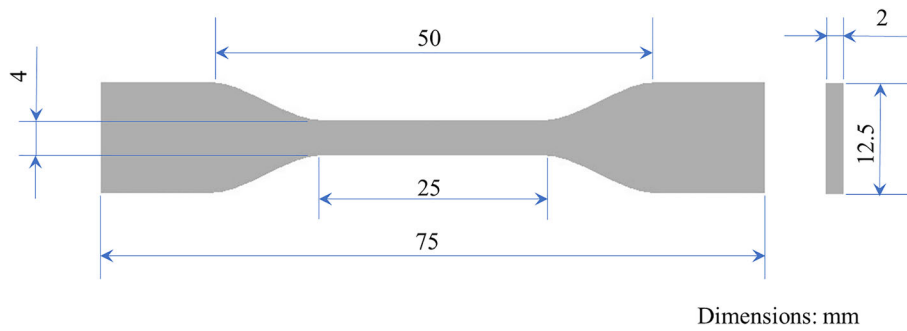
Dimensions: mm

Fig. 2 CAD of tensile test specimens dimensions based on ASTM standard (D638)

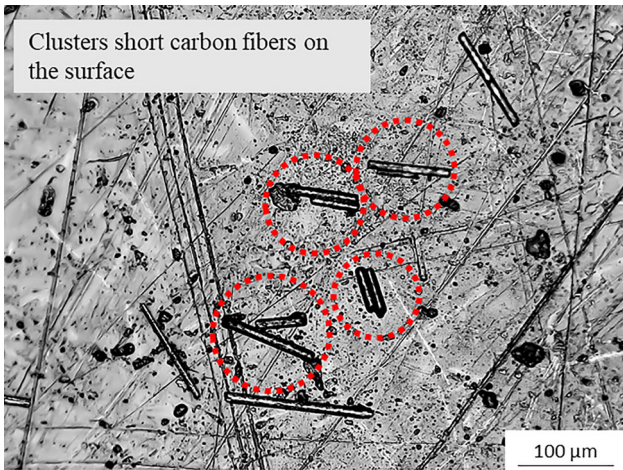Clusters short carbon fibers on the surface

100 μm

Fig. 3 Cluster carbon fiber powder on the superior surface (last printed layer) of the test specimen with 1.5 wt.%

challenges in dispersion due to its relatively large specific surface area. As depicted in Fig. 3, clusters of short carbon fibers pose difficulties in achieving uniform dispersion within the resin matrix.

To address this issue, several measures were taken, including increasing the mechanical agitation time and immersing the printed specimens in an isopropanol solution. The extended mechanical agitation time allows for better dispersion and separation of the short carbon fiber, promoting more dispersion and distribution within the resin. Immersion in the isopropanol solution helps in removing any residue from the short carbon fiber and mechanical agitation helps in better dispersion and distribution of the short carbon fiber throughout the composite material. This same mechanical agitation was responsible for the breakage in length of some short carbon fiber. The steps were taken to improve the interfacial bond and overall mechanical performance of the composites.

The breakage of carbon fibers was induced by the geometry and high viscosity of the resin used in the study, resulting in a reduction in length during the printing of the test specimens. This breakage was beneficial as it reduced fiber sedimentation, especially at concentrations below 15 wt.%. However, concentrations above this limit led to significant sedimentation, hindering resin photopolymerization and compromising print quality.

The increase in resin viscosity (500 mPa.s) and carbon fiber concentration is likely to result in an increased formation of voids within the composite material. This is attributed to the

UV resin's challenge in fully infiltrating the surfaces of the carbon fibers. These voids adversely affect the mechanical properties and durability of the composite material, serving as initiation points for cracks and facilitating moisture penetration, thereby contributing to material anisotropy. Figure 4 illustrates the void volume for each wt.% of short carbon fiber, as per ASTM D2734.

The microscopic examination of the printed and cleaned specimens using an Olympus BX51TF microscope revealed the dispersion and distribution of short carbon fiber within the UV-curable resin. It was observed that the short carbon fiber had good dispersion and distribution in the in-plane direction for each weight percentage (wt.%) of carbon fiber specimens (as shown in Fig. 5), and no sedimentation was observed. The short carbon fiber appeared as white cylindrical structures under the microscope.

3.2 Density

The weight percentage (wt.%) of short carbon fiber has an impact on the final density of the composite specimens. Comparing the pure resin with the 15 wt.% short carbon fiber, there was a density reduction of 16% in the final printed specimens. On average, each 3 wt.% increase in short carbon fiber content led to a density reduction of 0.01 g/cm^3. Figure 6 illustrates the final densities of the specimens for each weight percentage of short carbon fiber.

Indeed, the reduction in density of the specimens cannot be solely attributed to the increase in short carbon fiber. Other factors may contribute to this density reduction, such as the formation of voids around the short carbon fiber due to incomplete resin adhesion or the relatively lighter density of the short carbon fiber compared to the UV-curable resin.

3.3 Hardness

The hardness of fiber-reinforced composite samples is influenced by various factors, including the type and arrangement of fibers, the percentage fraction of fibers, the hardness of the base resin, and the bonding between fibers and the base material. Surface hardness of the last printed layer, specifically, did not exhibit significant changes with varying concentrations of short carbon fiber, as illustrated in Fig. 7, which presents average hardness values (Shore D) for the printed specimens. This observation suggests that the incorporation of short carbon fiber into the UV-curable resin matrix had no pronounced impact on the surface hardness of the specimens. Consistent with findings reported by Hu et al. (Ref 18), there was a lack of change in surface hardness with increasing reinforcement in the
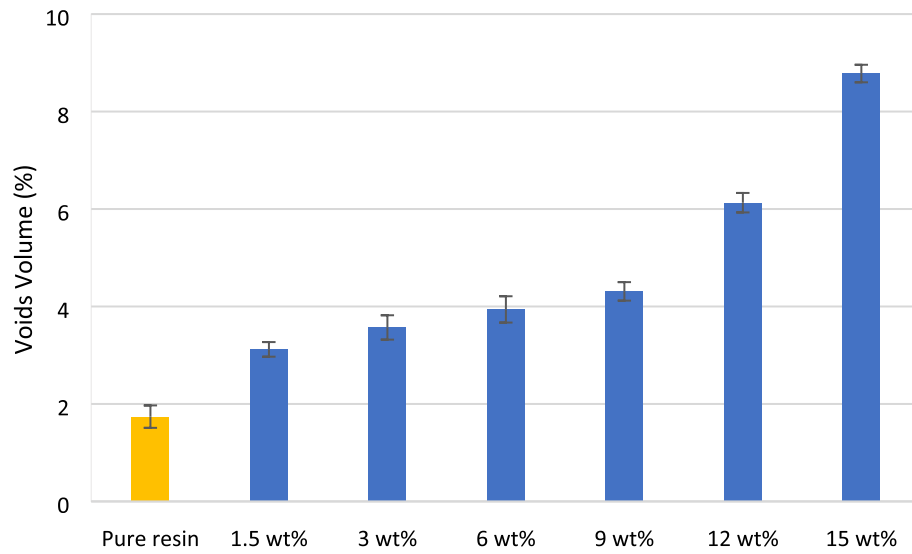
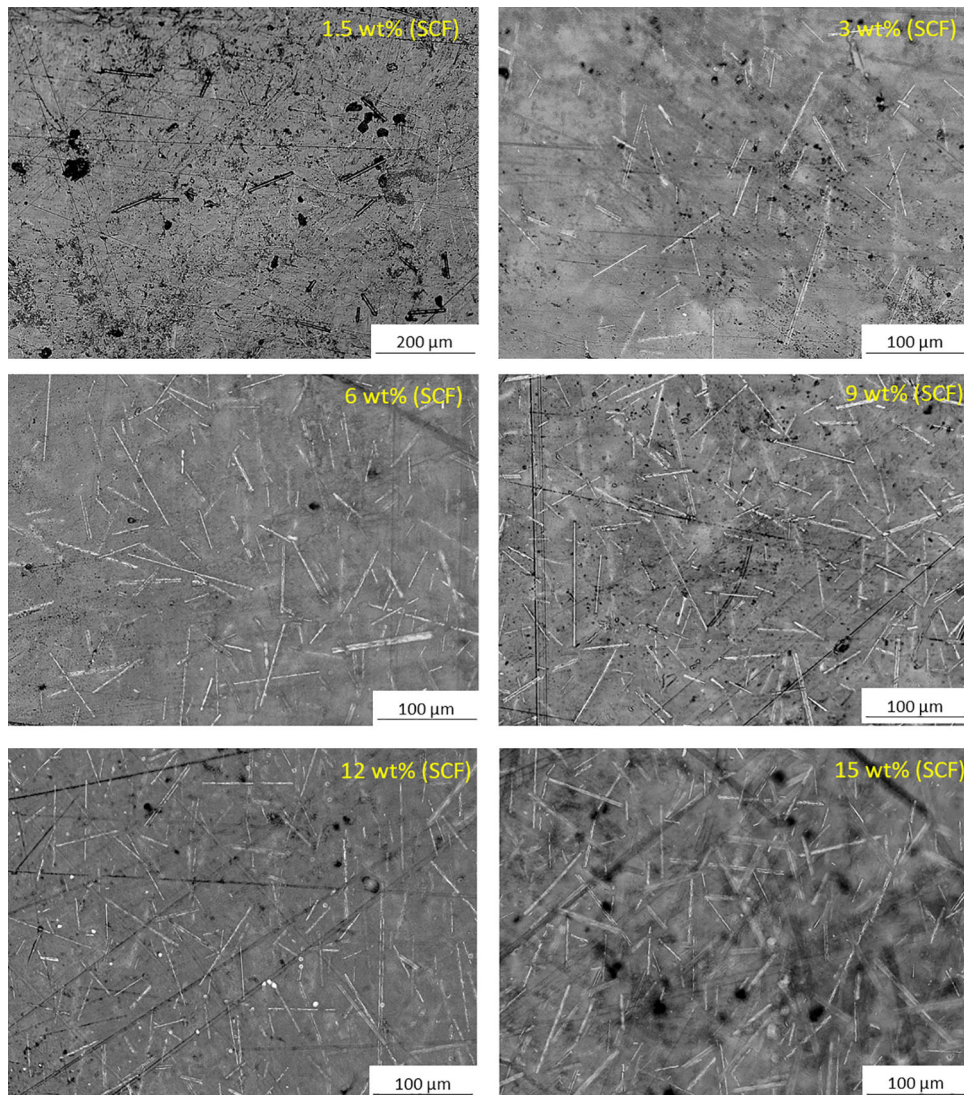**Fig. 4** Voids volume (%) void volume for each wt.% of short carbon fiber

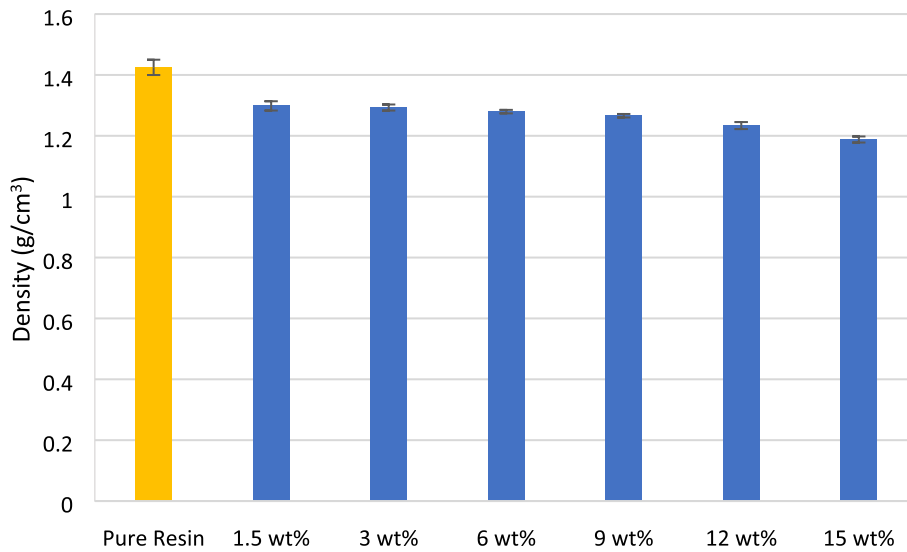**Fig. 5** Dispersion and distribution of each wt.% of short carbon fiber along the thickness of the test specimens

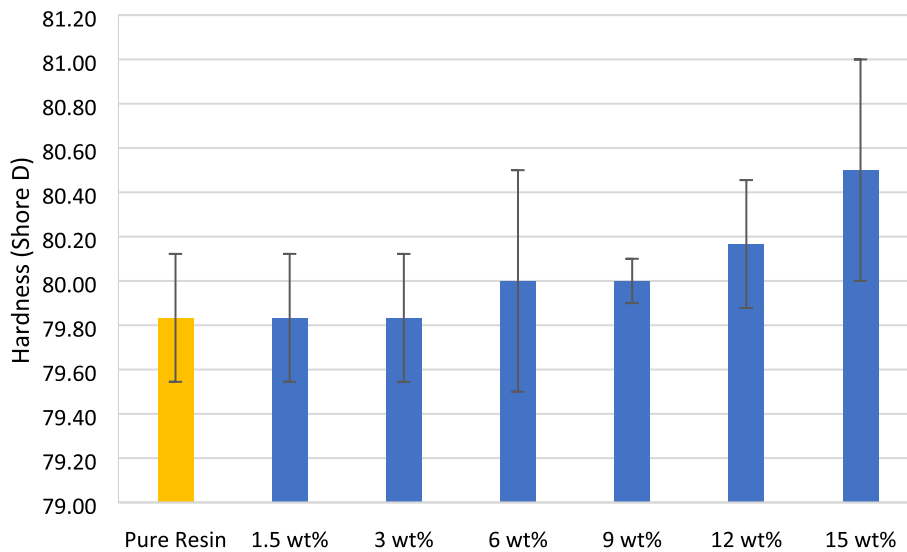**Fig. 6** Influence of the weight percentage of short carbon fiber on the density of the test specimens

Fig. 7 Comparison of the weight percentage of short carbon fiber and its effect on the hardness of the test specimens

matrix. However, incremental percentages of short carbon fibers were observed to contribute to a marginal increase in hardness. This phenomenon is attributed to the effective distribution and dispersion of short carbon fibers, leading to enhanced interfacial bonding between the UV resin and short carbon fibers.

3.4 Surface Roughness

The surface roughness value (Ra) exhibited an average increase of 0.02 μm, demonstrating an almost linear relationship with the amount of short carbon fiber added. Figure 8 illustrates the progression of surface roughness (Ra) of the specimens as a function of the percentage of short carbon fiber. This indicates that as the concentration of short carbon fiber increased, the surface roughness of the specimens also increased in a relatively consistent manner.

The surface roughness can indeed serve as a valuable indicator of printing accuracy, and the obtained values suggest that the manufactured specimens exhibit a satisfactory level of

accuracy (Ref 13). This indicates that the LCD 3D printing process, including the incorporation of various weight percentages of short carbon fiber, allows for the production of complex 3D shapes with a reasonable level of precision and fidelity.

Furthermore, the ability to manufacture complex 3D shapes using different weight percentages of short carbon fiber highlights the versatility and potential of DLP 3D printing technology. This opens up possibilities for creating structurally enhanced and tailored composite parts with desired mechanical properties by adjusting the short carbon fiber content.

3.5 Mechanical Properties

The investigation focused on the force, Young's modulus, tensile strength, and maximum extension of specimens made from pure resin as well as varying weight percentages (wt.%) of short carbon fiber. These properties are crucial for design information, as they depend on the intended application and desired material performance.
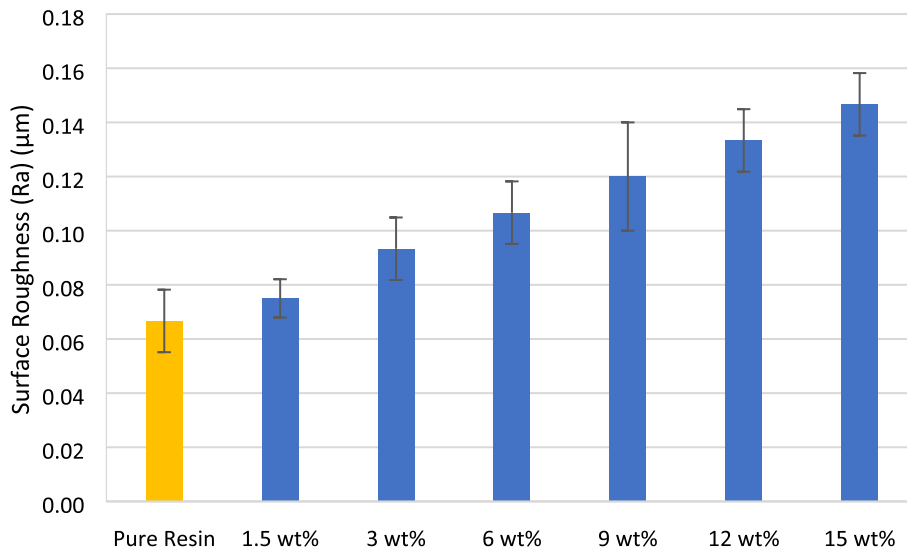
Fig. 8 Influence of the weight percentage of short carbon fiber on the surface roughness of the test specimens
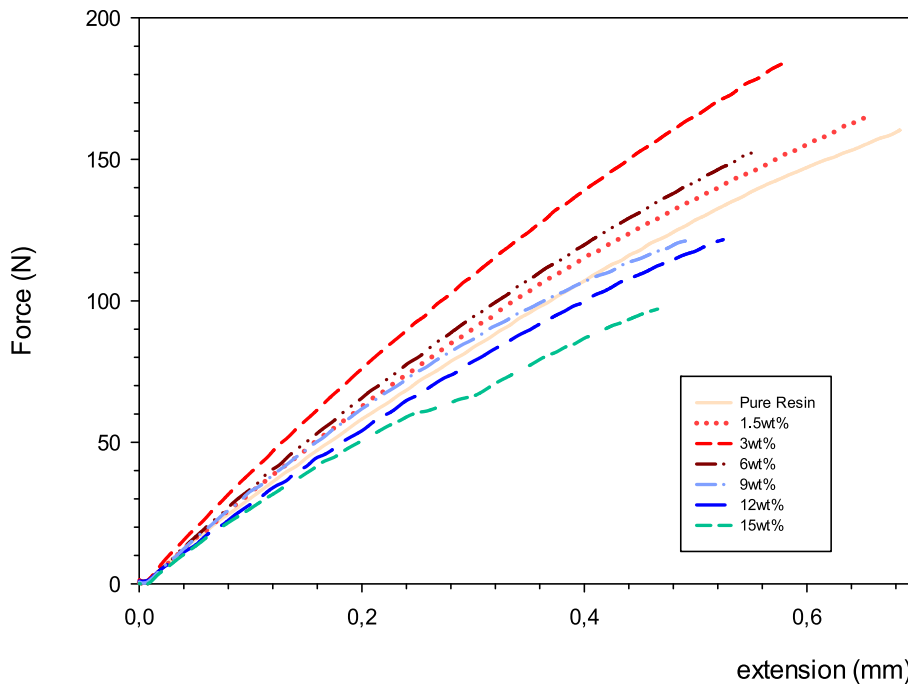

Fig. 9 Load versus extension for pure resin and all wt.%

Figure 9 illustrates typical load versus extension curves, which are derived from the average of the five tests conducted. The load versus extension behavior of both the pure resin and all weight percentages of short carbon fiber specimens exhibited linearity up to their respective maximum breaking loads. There were no visible indications of damage initiation or specific damage loads observed for either the pure resin or the short carbon fiber specimens.

It is evident from Fig. 8 that all specimens exhibited a brittle failure behavior. This type of brittle failure can impose limitations on their utilization in critical applications such as aerospace, automotive, and marine sectors, unless their failure behavior, particularly stress concentrations, are addressed and mitigated.

In terms of extension (deformation), the pure resin exhibited a higher value (0.683 mm) compared to the composites containing various weight percentages of short carbon fiber. The incorporation of short carbon fiber led to a reduction in the extension (deformation) of the specimens. On average, each 3 wt.% increase in short carbon fiber content resulted in a decrease in specimen extension of 0.03 mm.

Regarding the force applied during the tensile tests, there was a significant increase in force for the concentrations ranging from 1.5 to 3 wt.%. Particularly, at 3 wt.% short carbon fiber concentration, the maximum force reached (184.84 N) was 13.3% higher than that of the pure resin (160.21 N). This percentage resulted in effective transfer of load and consequently improved strength. This behavior of force evolution as
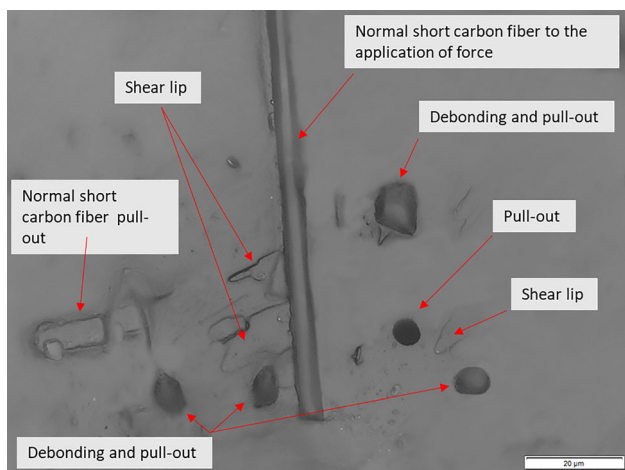
Fig. 10 Failures modes observed on the surface fracture of specimen with 15 wt % short carbon fiber

a function of the percentage of reinforcement contraction in the matrix was also observed in the study by Yukako et al. (Ref 12).

However, above 3 wt.% short carbon fiber concentration, the effect of increasing the concentration had the opposite effect, leading to a reduction in the maximum force. Among the different concentrations above 3 wt.%, the most significant reductions, averaging 20%, occurred between the concentrations of 6 to 9 wt.% and 12 to 15 wt.%. A possible reason for the decrease in force, starting from 3 wt.%, is the increase in the bond length between the carbon fibers powder and the resin, promoting a greater concentration of stresses responsible for the origin of the triaxial stresses around the fibers, while leading to debonding. In addition, fiber pull-out also increases, which also acts as stresses triaxiality at these locations and thus induces crack initiation.

To investigate and validate these statements, a microscopic analysis of the fracture region of a specimen with a 15 wt.% short carbon fiber concentration was performed. The results of this analysis are depicted in Fig. 10, providing visual evidence of the fracture surface and allowing for further examination of the distribution and interfacial bonding between the resin matrix and the short carbon fiber.

In composites, debonding and pull-out are mechanisms present from the beginning to the final fracture. In Fig. 9, there are shear lips, which confirms that the fracture (crack propagation) is not in plane strain condition.

The normal alignment of the short carbon fibers to the direction of the applied force resulted in a brittle fracture behavior. When the force is applied perpendicular to the carbon fibers, it creates stress concentrations along their length. This can lead to localized failure and brittle fracture within the material (Ref 19).

The orientation of the short carbon fiber powders becomes particularly significant in determining the mechanical properties and failure mode of the composite material. To improve the overall strength and ductility of the specimens, it would be important to ensure proper alignment and orientation of the carbon fibers to minimize stress concentrations and enhance load transfer within the material.

These findings demonstrate the complex interplay between short carbon fiber content, extension (deformation), and

maximum force in the specimens, highlighting the importance of carefully optimizing the composite composition for desired mechanical properties.

Figure 11 illustrates the resulting Young's modulus values, while Fig. 12 depicts the tensile strength values of all specimens. The data confirms that there is an increase in Young's modulus and tensile strength up to 3 wt.% short carbon fiber content. For example, Young's modulus increased from 1.867 GPa (pure resin) to 2.571 GPa (3 wt.%), representing a 27% increase.

These findings suggest that the incorporation of short carbon fiber up to a certain concentration enhances the mechanical properties of the composite. However, it is crucial to carefully determine the optimal weight percentage of short carbon fiber to achieve the desired improvement in Young's modulus and tensile strength.

The results of the tensile test varied depending on the carbon fiber wt.% and the dispersity, with some demonstrating a remarkable improvement in Young's modulus and tensile strength and others showing a drop in Young's modulus and tensile strength compared to the specimen printed without short carbon fiber (pure resin). The resulting Young's modulus and tensile strength of all specimens are shown in Figs. 11 and 12, respectively. The values confirmed that with an increase up to 3 wt.% short carbon fiber), Young's modulus and tensile strength increase. Young's modulus increased from 1,867 GPa (pure resin) to 2,571 GPa (3 wt.%), an increase of 27%.

Indeed, for the 3 wt.% concentration of short carbon fiber, there was a notable increase in the tensile strength values compared to the pure resin. The pure resin exhibited a tensile strength of 18 MPa, whereas the 3 wt.% short carbon fiber composite demonstrated a tensile strength of 32 MPa. This represents a significant increase of 44% in tensile strength. The study conducted by Salih et al. (Ref 23) also reported the presence of an optimal concentration the carbon fiber, leading to the attainment of peak values for both the modulus of elasticity and maximum tensile strength.

The enhancement in tensile strength highlights the reinforcing effect of the short carbon fiber within the composite material. The presence of carbon fibers can improve the load-bearing capacity and overall strength of the material, resulting in increased tensile strength. This demonstrates the potential of carbon fiber-reinforced composites for applications requiring high strength and structural performance.

For the 3 wt.% concentration of short carbon fiber, there was a significant increase in the tensile strength values when compared to the pure resin. The pure resin showed a tensile strength of 18 MPa while for 3 wt.% the tensile strength was 32 MPa, an increase of 44%. This percentage resulted in effective transfer of load and consequently improved strength.

Indeed, the increase in weight percentage (wt.%) of short carbon fiber significantly influences the extensions (deformations), Young's modulus, and tensile strength of the specimens. The dispersion and distribution of short carbon fiber within the photopolymeric resin matrix, along with the increased number of carbon fibers, can affect these properties.

Figure 13 presents the toughness of the prepared composite materials. The toughness, which is a measure for absorbing energy, increased by 33% (from 14.21 MPa to 21.18 MPa) when short carbon fiber was increased from 0 to 3 wt.%, implying the positive effect of the addition. This behavior can occur because the short carbon fiber promotes only partial
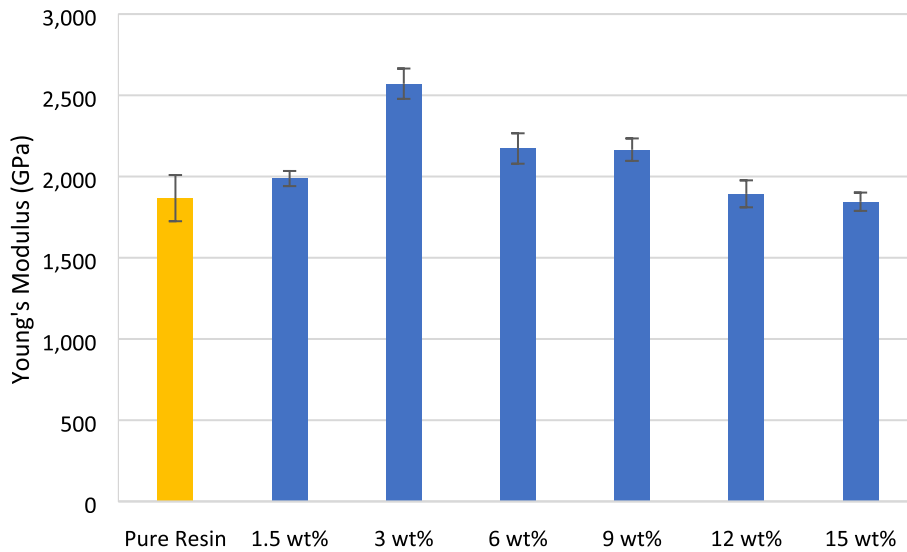
Fig. 11 Young's modulus of 3D printed composites specimens as a function of wt.% short carbon fiber
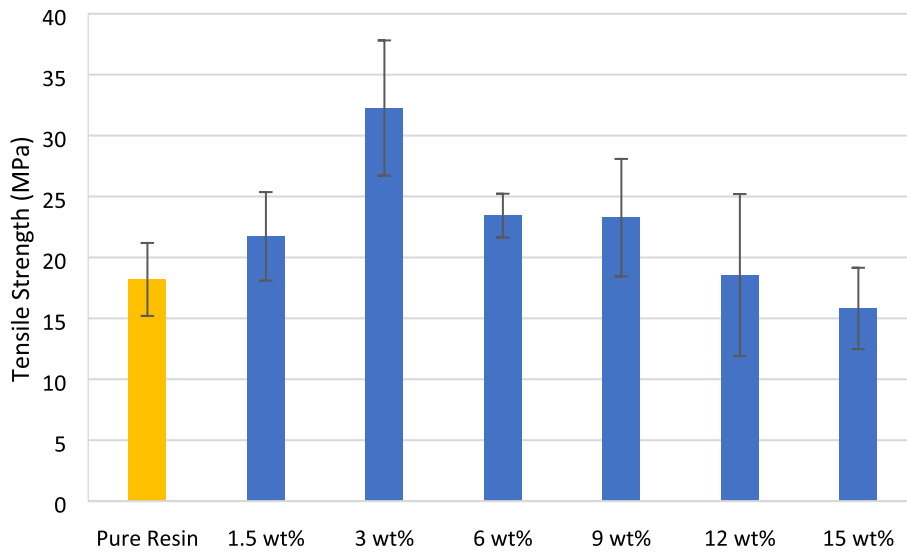

Fig. 12 Tensile strength of 3D printed composites specimens as a function of wt.% short carbon fiber

stress within pure resin, changing the direction of crack development.

The increase in toughness value until the short carbon fiber concentration reaches a certain level (in this case, 3 wt.%) followed by a decrease when the short carbon fiber concentration is increased further can be explained based on the deboning mechanism. In this mechanism, voids are created between the short carbon fiber/resin matrix interface, leading to shear yielding in the composite, which can only toughen the material to a certain level.

4. Conclusions

- Dispersion and distribution of short carbon fiber within the resin matrix, as well as the weight percentage of short carbon fiber, have a significant impact on the mechanical properties of the composites.
- Measures were taken to address the aggregation issue,

including increased mechanical agitation time and immersion in an isopropanol solution, resulting in better dispersion and distribution of short carbon fiber within the composites.
- The weight percentage of short carbon fiber has a notable influence on the final density of the composites, with each 3 wt.% increase leading to a density reduction of 0.01 g/cm^3.
- The concentration of short carbon fiber did not significantly affect the surface hardness of the printed specimens.
- Surface roughness exhibited an average increase of 0.02 μm with increasing short carbon fiber content, indicating a linear relationship between the two.
- The incorporation of short carbon fiber up to a certain concentration enhances the Young's modulus and tensile strength of the composite.
- The concentration of 3 wt.% short carbon fiber showed a notable increase in tensile strength (44%) compared to the
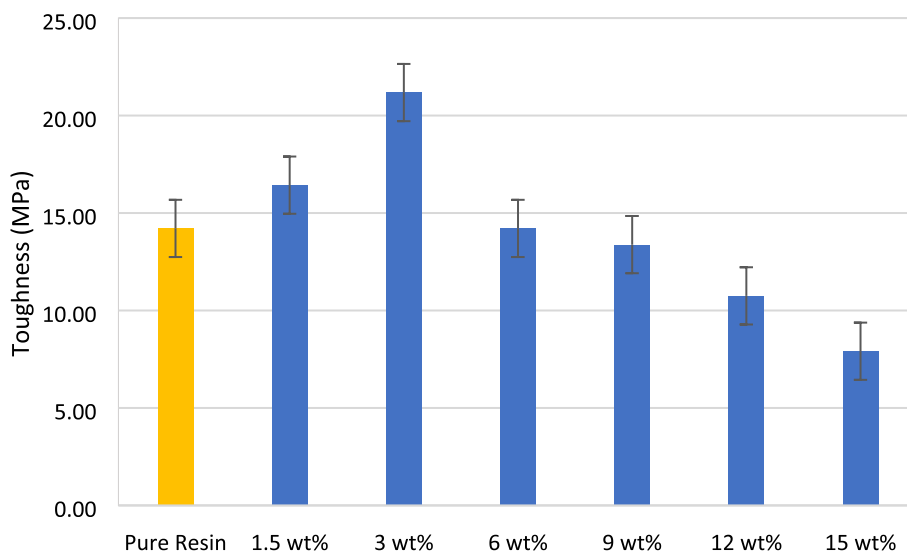
Fig. 13 Toughness of 3D printed composites specimens as a function of wt.% short carbon fiber

pure resin, highlighting the reinforcing effect of carbon fibers.

• The increase in weight percentage of short carbon fiber significantly influences extensions (deformations), Young's modulus, and tensile strength of the specimens, with dispersion and distribution of short carbon fiber playing a key role in these properties.

Overall, the study demonstrates the potential of LCD 3D printing technology to manufacture composites with improved mechanical properties, with careful optimization of short carbon fiber content being essential to achieve the desired performance.

Acknowledgments

References

1. A. Jacob. Building Confidence in Recycled Carbon Fiber|CompositesWorld. Available online: https://www.compositesworld.com/articles/building-confidence-in-recycled-carbon-fiber (accessed on 28 June 2023)
2. S.K. Gopalraj and T. Karki, A Review on the Recycling of Waste Carbon Fibre/Glass Fibre-Reinforced Composites: Fibre Recovery, Properties and Life-Cycle Analysis, *SN. Appl. Sci.*, 2020, **2**, p 433
3. J. Zhang, V.S. Chevali, H. Wang, and C.H. Wang, Current status of Carbon Fibre and Carbon Fibre Composites Recycling, *Compos. B Eng.*, 2020, **193**, 108053
4. J. Sloan, *The Outlook for Carbon Fibre Supply and Demand*, Composites World Gardner Bussines Media Inc., USA, 2021
5. A. Isa, N. Nosbi, M.C. Ismail, H.M. Akil, W.F.F.W. Ali, and M.F. Omar, A Review on Recycling of Carbon Fibres: Methods to Reinforce and Expected Fibre Composite Degradations, *Materials*, 2022, **15**, p 4991
6. L. Giorgini, T. Benelli, L. Mazzocchetti, C. Leonardi, G. Zattini, G. Minak, E. Dolcini, C. Tosi, and I. Montanari, Pyrolysis as a Way to Close a CFRC Life Cycle: Carbon Fibers Recovery and Their Use as Feedstock for a New Composite Production, *AIP Conf. Proc.*, 2014, **1599**, p 354–357
7. B. Newman, C. Creighton, L.C. Henderson, and F. Stojcevski, A review of Milled Carbon Fibres in Composite Materials, *Compos. Part A: Appl. Sci. Manufact.*, 2022, **163**, p 107249. https://doi.org/10.1016/j.compositesa.2022.107249
8. D.J. Eyckens, F. Stojcevski, A. Hendlmeier, J.D. Randall, D.J. Hayne, M.K. Stanfield et al., Carbon Fibre Surface Chemistry and its Role in Fibre-To-Matrix Adhesion, *J Mater Chem A*, 2021, **9**, p 26528–26572
9. J.D. Randall, D.J. Eyckens, E. Sarlin, S. Palola, G.G. Andersson, Y. Yin et al., Mixed Surface Chemistry on Carbon Fibers to Promote Adhesion in Epoxy and PMMA Polymers, *Ind. Eng. Chem. Res.*, 2022, **61**, p 1615–1623
10. S. He, D. Carolan, A. Fergusson, and A.C. Taylor, Toughening Epoxy Syntactic Foams with Milled Carbon Fibres: Mechanical Properties and Toughening Mechanisms, *Mater. Des.*, 2019, **169**, 107654
11. S. Karimi and S. Javadpour, Comparison of the Role of Milled Glass and Carbon Fibers on Mechanical Properties of (bisphenol A)-Based Epoxy Composites, *J. Vinyl Add. Tech.*, 2018, **24**, p 130–138. https://doi.org/10.1016/j.addma.2018.10.033
12. S. Yukako, M. Ryosuke, U. Masahito, T. Akira, and Y. Hirano, 3D Printing of Discontinous and Continous Fibre Composites Using Stereolithography, *Addit. Manuf.*, 2018, **24**, p 521–527
13. T. Yamamoto, Y. Makino, and K. Uematsu, Improved Mechanical Properties of PMMA Composites: Dispersion, Diffusion and Surface Adhesion of Recycled Carbon Fiber Fillers from CFRP with Adsorbed Particulate PMMA, *Adv. Powder Technol.*, 2017, **28**, p 2774–2778
14. D.J. Eyckens, J.D. Randall, F. Stojcevski, E. Sarlin, S. Palola, M. Kakkonen et al., Examining Interfacial Interactions in a Range of Polymers Using Poly(Ethylene Oxide) Functionalized Carbon Fibers, *Compos. A Appl. Sci. Manuf.*, 2020, **138**, 106053
15. J.W. Lee, S.J. Park, and Y.H. Kim, Effect of Milled Carbon on Interfacial Properties of Carbon Fiber Reinforced Epoxy-Based Composites, *Int. J. Mod. Phys. B*, 2018, **32**, p 1840082
16. H. Katogi and K. Takemura, Flexural Property and In Situ Observation of Carbon Milled Fiber Added Plain Woven Carbon Fiber/Epoxy Resin Composite, *Key Eng. Mater.*, 2016, **665**, p 57–60
17. K. Rahmani, G. Wheatley, A. Sadooghi, S.J. Hashemi, and J. Babazadeh, The Experimental Investigation of Hardness and Wear Behaviors of Inner Surface of the Resin Tubes Reinforced By Fibers, *Results Eng.*, 2021, **11**, 100273
18. K.B. Mahat, I. Alarifi, A. Alhari, and R. Asmatulu, Effects of UV Light on Mechanical Properties of Carbon Fiber Reinforced PPS Thermoplastic Composites, *Macromol. Symp.*, 2016, **365**(1), p 157–168. https://doi.org/10.1002/masy.201650015

19. H. Eng, S. Maleksaeedi, S. Yu, Y.Y.C. Choong, F.E. Wiria, C.L.C. Tan, P.C. Su, and J. Wei, 3D Stereolithography of Polymer Composites Reinforced with Orientated Nanoclay, *Proc. Eng.*, 2017, **216**, p 1–7

20 H.Q. Hu, L. Zhao, J.Q. Liu, S.B. Wen, Y.J. Gu, Y.K. Zhang, H.T. Wang, and L.Y. Zhang, Carbon Fiber Reinforced Epoxy Composites Used for Rapid Tooling, *Adv. Mater. Res.*, 2011, **287–290**, p 197–200

21 S.T. Cholake, G. Moran, B. Joe, Y. Bai, R.R. Singh, X.L. Zhao, S.H. Rizkalla, and S. Bandyopadhyay, Improved Fracture Toughened Epoxy Matrix System Reinforced with Recycled Milled Carbon Fibre, *Ann. Mater. Sci. Eng.*, 2015, **2**, p 1–10

22. D. He, V.K. Soo, H.C. Kim, P. Compston, and M. Doolan, Comparative Life Cycle Energy Analysis of Carbon Fibre Pre-Processing, Processing and Post-Processing Recycling Methods, *Resour. Conserv. Recycl.. Conserv. Recycl.*, 2020, **158**, 104794

23. R.M. Salih, A. Kadauw, H. Zeidler, and R. Aliyev, Investigation of LCD 3D Printing of Carbon Fiber Composites by Utilising Central Composite Design, *J. Manufact. Mater. Process.*, 2023, **7**, p 58